IOPscience iopscience.iop.org

Home Search Collections Journals About Contact us My IOPscience

Visible photoluminescence from chain $Tl_4In_3GaSe_8$ semiconductor

This article has been downloaded from IOPscience. Please scroll down to see the full text article.

2006 J. Phys.: Condens. Matter 18 6057

(http://iopscience.iop.org/0953-8984/18/26/023)

View the table of contents for this issue, or go to the journal homepage for more

Download details:
IP Address: 129.252.86.83
The article was downloaded on 28/05/2010 at 12:00

Please note that terms and conditions apply.

INSTITUTE OF PHYSICS PUBLISHING JOURNAL OF PHYSICS: CONDENSED MATTER

J. Phys.: Condens. Matter **18** (2006) 6057–6064 doi:10.1088/0953-8984/18/26/023

Visible photoluminescence from chain $Tl_4In_3GaSe_8$ semiconductor

N M Gasanly[1] **and K Goksen**

Department of Physics, Middle East Technical University, 06531 Ankara, Turkey

E-mail: nizami@metu.edu.tr

Received 5 April 2006, in final form 3 May 2006
Published 19 June 2006
Online at stacks.iop.org/JPhysCM/18/6057

Abstract

The emission band spectra of undoped $Tl_4In_3GaSe_8$ chain crystals have been studied in the 16–300 K temperature range and the 535–740 nm wavelength range. Two visible photoluminescence bands centred at 589 and 633 nm were observed at $T = 16$ K. Variations of both bands have been investigated over a wide range of laser excitation intensity (3×10^{-4}–1.2 W cm^{-2}). Radiative transitions with energies of 2.10 and 1.96 eV from two upper conduction bands to two shallow acceptor levels (0.03 and 0.01 eV), respectively, were suggested as being responsible for the observed bands in $Tl_4In_3GaSe_8$ crystal, which is non-transparent in the visible range.

1. Introduction

The compound $Tl_4In_3GaSe_8$ belongs to the group of semiconductors with a chain structure. This crystal is a structural analogue of $TlInSe_2$, in which a quarter of the trivalent indium atoms are replaced by gallium atoms [1, 2]. In the lattice of the $Tl_4In_3GaSe_8$ crystal, indium (gallium) atoms are each surrounded by four selenium atoms and form chains along the tetragonal c-axis. These chains are connected to each other by univalent thallium atoms (figure 1).

The photoelectric and optical properties of $TlInSe_2$ crystals were studied in [3–8]. The fundamental absorption edge is formed by indirect and direct transitions with $E_{gi} = 1.07$–1.23 eV and $E_{gd} = 1.27$–1.44 eV, respectively [3–5]. Among the useful properties of $TlInSe_2$ crystals are negative differential resistance with S-type current–voltage characteristics [3] and high thermoelectric power [9]. For $Tl_4In_3GaSe_8$ single crystals, the value of the indirect band gap, $E_{gi} = 0.94$ eV, has been evaluated from transmittance and reflectance measurements [2]. Recently, band structure calculations have been reported for isostructural $TlInSe_2$, $TlInTe_2$ and $TlGaTe_2$ chain crystals [10–13]. For the latter crystal, from a angle-resolved photoemission study, a strong temperature-dependent shift of the Fermi level was ascertained [13].

[1] Author to whom any correspondence should be addressed. On leave from: Physics Department, Baku State University, Baku, Azerbaijan.

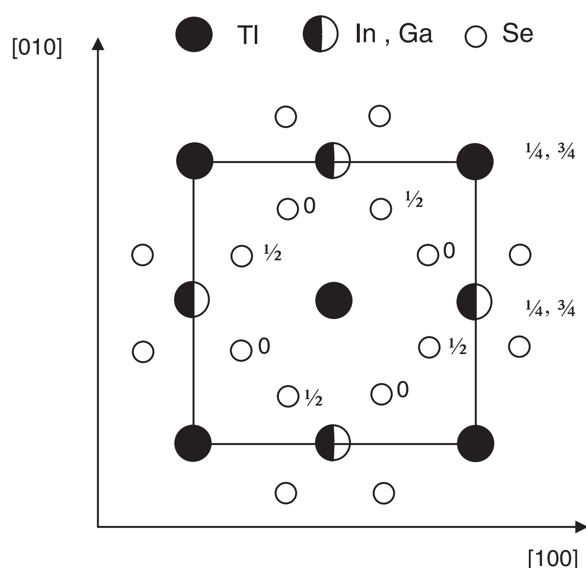

Figure 1. Projection of the unit cell of $Tl_4In_3GaSe_8$ crystal on the (001) plane. The figures indicate heights above this plane.

In the present paper, we report the results of photoluminescence (PL) investigations in the 535–740 nm wavelength and 16–300 K temperature regions for $Tl_4In_3GaSe_8$ crystals. The intensity change of the PL emission bands with excitation laser intensity was also studied. Analysis of the data suggests that the radiative transitions originate from the recombination of charge carriers from free to bound states. Finally, a scheme for the energy states taking part in the observed PL is proposed.

2. Experimental details

Single crystals of $Tl_4In_3GaSe_8$ were grown by the Bridgman method from a stoichiometric melt of starting materials sealed in evacuated (10^{-5} Torr) silica tubes with a tip at the bottom. The resulting ingots (grey-black in colour) showed good optical quality and were easily cleaved along two mutually perpendicular planes which are parallel to the *c*-axis of the crystal. The chemical composition of $Tl_4In_3GaSe_8$ crystals was determined by energy-dispersive spectroscopic analysis (EDSA) using a JSM-6400 scanning electron microscope (figure 2). The composition of the studied samples (Tl:In:Ga:Se) was found to be 25.5:19.1:6.5:48.9, respectively. Moreover, EDSA indicates that carbon, oxygen and silicon impurities are present in $Tl_4In_3GaSe_8$ crystals. The analysis of x-ray powder diffraction data showed that $Tl_4In_3GaSe_8$ crystallizes in a tetragonal unit cell with lattice parameters $a = 0.8066$ and $c = 0.6697$ nm [2]. These values are close to the values of $a = 0.8075$ and $c = 0.6847$ nm reported for $TlInSe_2$ crystal [1].

The samples for PL measurements were freshly and gently cleaved with a razor blade from the middle part of the grown ingots and no further polishing and cleaning treatments were required because of the natural mirror-like cleavage planes. Typical dimensions of the samples obtained were $9 \times 2 \times 1$ mm^3. The electrical conductivity of the sample studied was p-type, as determined by the hot probe method. The green line ($\lambda = 532$ nm) of a continuous frequency-doubled YAG:Nd^{3+} laser and the red line ($\lambda = 632.8$ nm) of a He–Ne laser were used as the

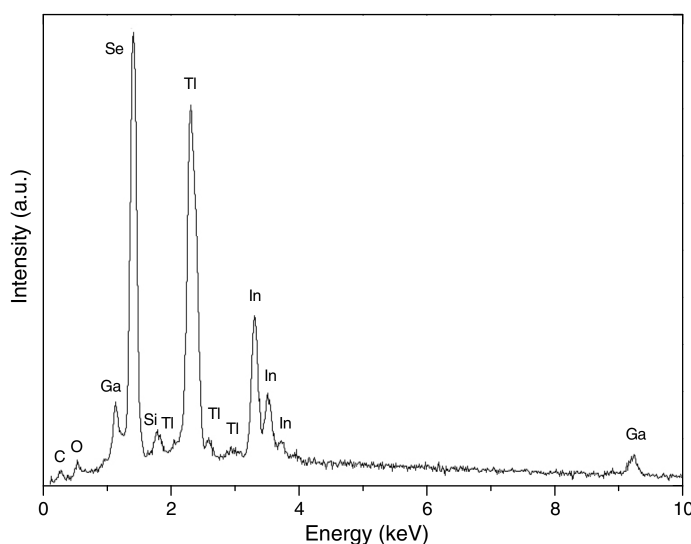

Figure 2. Energy-dispersive spectroscopic analysis of $Tl_4In_3GaSe_8$ crystal.

excitation light sources. PL experiments were carried out by collecting the light from the laser-illuminated face of the sample in a direction close to the normal of the c-axis. A closed-cycle helium cryostat was used to cool the sample from room temperature down to 16 K, and the temperature was controlled within an accuracy of ±0.5 K. The PL spectra of the sample in the region 535–740 nm were measured using an Oriel MS257 monochromator with a grating of 1200 grooves mm^{-1} and 3.22 nm mm^{-1} dispersion, and a Hamamatsu S7010-1008 FFT-CCD Image Sensor with a single-stage electric cooler. The resolution of the PL experimental system was better than 3 meV. Sets of neutral density filters were used to adjust the laser excitation intensity from 0.0003 to 1.1777 W cm^{-2}. The PL spectra have been corrected for the spectral response of the optical apparatus. All the spectra have been analysed by using a fitting program 'Peak Fit for Win 32 Version 4'. PL bands were fitted by Gaussian profiles. The procedure yields the peak position, short- and long-wavelength side half-widths, and the intensity of the bands. In the case of coexisting bands, we applied the same program to deconvolute the observed bands.

3. Results and discussion

The PL spectra of $Tl_4In_3GaSe_8$ crystals comprise two emission bands (labelled as A and B) dominating at different excitation intensities. For the analysis, we plotted two figures to trace the behaviour of the PL bands with respect to laser excitation intensity variations at $T = 30$ K. Figures 3(a) and (b) show the PL spectra (B- and A-bands) measured in the 0.0003–0.0873 and 0.0873–1.1777 W cm^{-2} excitation intensity ranges, respectively. We observed that the B-band intensity at the peak maximum increases with increasing excitation intensity from 0.0003 up to 0.0873 W cm^{-2}. However, when the laser excitation intensity exceeds the value 0.0873 W cm^{-2}, this behaviour changes drastically. While the A-band arises and starts to dominate the spectra, the intensity of the B-band decreases rapidly in magnitude. It should be noticed that the B-band emission peak shifts slightly towards higher energies with increasing excitation laser intensity, whereas the A-band emission peak does not show a significant change.

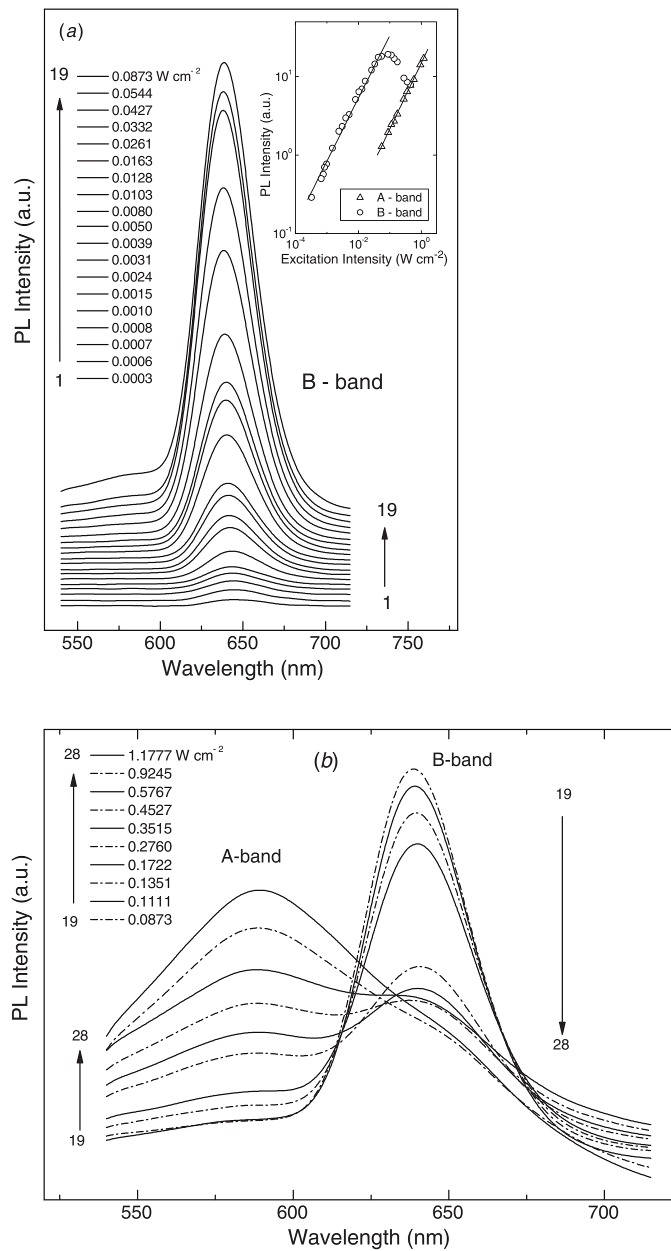

Figure 3. PL spectra of $Tl_4In_3GaSe_8$ crystal as a function of excitation laser intensity at $T = 30$ K: (a) B-band, 0.0003–0.0873 W cm^{-2} excitation intensity range (inset: dependences of PL intensities at the emission band maxima versus excitation laser intensity at $T = 30$ K—the solid lines show the theoretical fits using equation (1)); (b) A-band, 0.0873–1.1777 W cm^{-2} excitation intensity range.

To follow more thoroughly the behaviour of the A- and B-bands, we plotted the PL emission band maximum intensity versus excitation laser intensity on a logarithmic scale (inset of figure 3(a)). The common behaviour of both bands with respect to excitation laser intensity

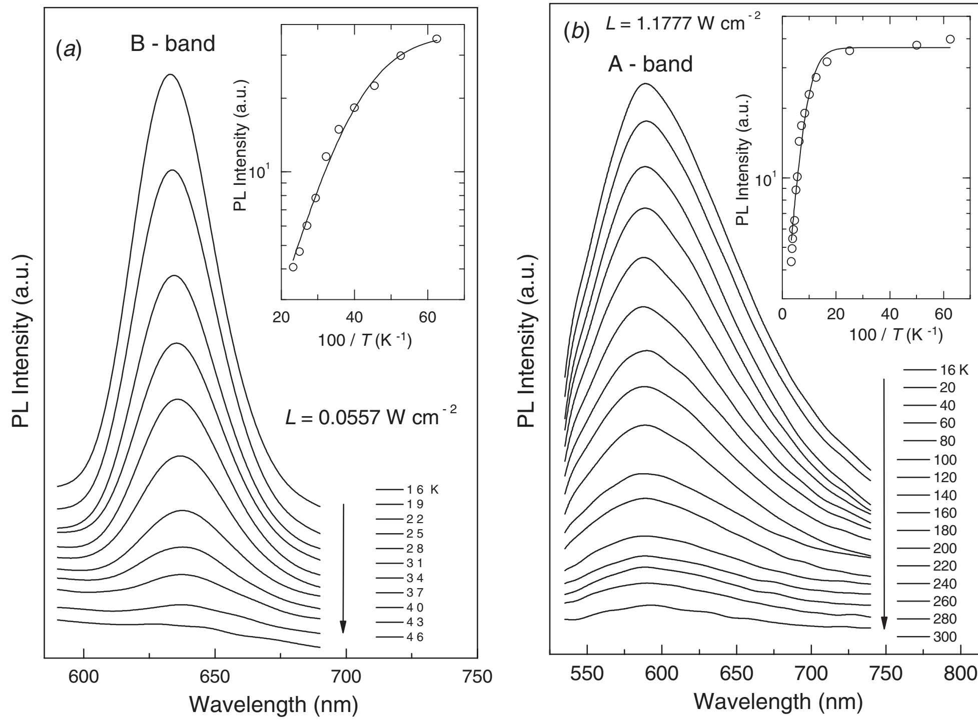

Figure 4. Temperature dependence of PL spectra from $Tl_4In_3GaSe_8$ crystals: (a) B-band, excitation laser intensity $L = 0.0557$ W cm^{-2} (inset: temperature dependence of PL band intensity)—circles are the experimental data and solid curve shows the theoretical fit using equation (2); (b) A-band, excitation laser intensity $L = 1.1777$ W cm^{-2} (inset: temperature dependence of PL band intensity)—circles are the experimental data and solid curve shows the theoretical fit using equation (2).

is clearly demonstrated by this graph. For the analysis, the experimental data for each band in the spectra (the linear part of the curves) were fitted by a power law of the form

$$I \alpha L^{\gamma}, \tag{1}$$

where I is the PL intensity at the emission band maximum, L is the excitation laser intensity, and γ is a dimensionless exponent. We find that the PL intensity for both bands increases sublinearly with increasing excitation laser intensity. By fitting the experimental data, we obtained the γ values as 0.84 and 0.80 for the A- and B-bands, respectively. For an excitation laser photon with an energy exceeding the band gap energy E_g, the exponent γ is generally $1 < \gamma < 2$ for the free- and bound-exciton emission and $\gamma \leqslant 1$ for free-to-bound and donor–acceptor pair recombination [14].

The dependence of the PL spectra on the temperature provides an important understanding of the nature and analysis of the luminescence spectra. To follow the temperature-dependent behaviour of both bands in the PL spectra of $Tl_4In_3GaSe_8$ crystals more clearly, we chose particular excitation intensities where each band is heavily dominant in the spectra, namely $L = 0.0557$ and 1.1777 W cm^{-2} for B- and A-band, respectively. The PL spectra (B-band) registered in the 590–690 nm wavelength and the 16–46 K temperature ranges are shown in figure 4(a). Figure 4(b) presents the PL spectra (A-band) measured in the 535–740 nm wavelength and 16–300 K temperature ranges. We observed that, at $T = 16$ K, the B- and A-bands were centred at 633 nm (1.96 eV) and 589 nm (2.10 eV), respectively. The emission

bands have asymmetrical Gaussian line shapes with short- and long-wavelength side half-widths of 0.172 and 0.261 eV (A-band) and 0.055 and 0.062 eV (B-band), respectively. As seen from the figures 4(a) and (b), both bands change their intensities and peak positions with temperature changes: the peak intensities decrease as the temperature is increased and the peak positions show several degrees of red shift with increasing temperature (about 5 and 1 nm for B- and A-bands, respectively). The observed behaviour of the peak energy positions for the A- and B-bands satisfies the temperature dependence expected for free-to-bound recombination [15, 16].

The experimental data for the temperature dependence of PL spectra for the A- and B-bands can be fitted by the following expression [17]:

$$I(T) = \frac{I_0}{1 + \alpha \exp(-E_t/kT)}, \tag{2}$$

where I_0 is a proportionality constant, E_t is the thermal activation energy, k is the Boltzman constant, and α is the recombination process rate parameter. The emission band maximum intensities with respect to reciprocal temperature are drawn in the insets of figures 4(a) and (b) in the 16–46 K (B-band) and 16–300 K (A-band) temperature ranges, respectively. After a nonlinear least-squares fit, the activation energies for the B- and A-bands are found to be 0.01 and 0.03 eV, respectively. These shallow levels can be considered as originating from uncontrolled impurities or from point defects due to deviations in stoichiometry. The former may be attributed to the presence of Si impurities introduced into $Tl_4In_3GaSe_8$ during the crystal growth process in ungraphatized ampoules (see figure 2).

Figure 5 shows the energy-level diagram for the PL emission bands of $Tl_4In_3GaSe_8$ crystal. Using the activation energies determined from the temperature dependence of the PL intensity for p-type $Tl_4In_3GaSe_8$ crystal, we placed acceptor levels $\boldsymbol{a}_1$ and $\boldsymbol{a}_2$ at 0.03 and 0.01 eV above the valence band. Taking into account the peak energy values of the observed transitions (2.10 and 1.96 eV for A- and B-bands, respectively), the related two initial energy states were then placed at 2.13 and 1.97 eV above the valence band.

The pseudo-potential method and tight binding model calculations of $TlInSe_2$ crystal band structure revealed the existence of several conduction bands [11, 18]. The top of the valence band and the bottoms of three lowest conduction bands (DCB I, DCB II, DCB III) are situated on the Brillouin-zone edge and belong to the irreducible representation T_3. In addition, the first conduction band has the second minimum (ICB) at the Brillouin-zone edge, which belongs to the irreducible representation D_1. Thus, the indirect band gap in $TlInSe_2$ crystal (1.28 eV) is formed by $T_3 \rightarrow D_1$ transitions. Three direct band gaps (0.60, 1.82 and 1.94 eV) correspond to $T_3 \rightarrow T_4$, $T_3 \rightarrow T_{10}$ and $T_3 \rightarrow T_6$ transitions, respectively [18]. According to [5], the direct transitions to the first conduction band (DCB I) in $TlInSe_2$ crystal is forbidden in the dipole approximation.

Taking into account the results of x-ray, transmission and photoluminescence measurements, we suppose, by analogy with the band structure calculation of $TlInSe_2$ [17], the existence in $Tl_4In_3GaSe_8$ crystal of an indirect band gap at 0.94 eV, and the second and third direct band gaps at 1.97 and 2.13 eV, respectively (figure 5). As for the first direct band gap, we could not observe this transition experimentally, since it is forbidden. Therefore, the assumed lowest conduction band (DCB I) is shown by a dotted curve in figure 5. The values of $\gamma = 0.84$ and 0.80, obtained from the dependence of the A- and B-band maximum intensities on excitation intensity, are in agreement with our assignment of the observed emission bands in $Tl_4In_3GaSe_8$ spectra to the free-to-bound recombination [14]. The assumption that the transitions from the minima of the third and second conduction bands to the acceptor levels $\boldsymbol{a}_1$ and $\boldsymbol{a}_2$, respectively, are responsible for the A- and B-emission bands is confirmed by the absence of these emission bands in the PL spectra of $Tl_4In_3GaSe_8$ crystal with excitation by

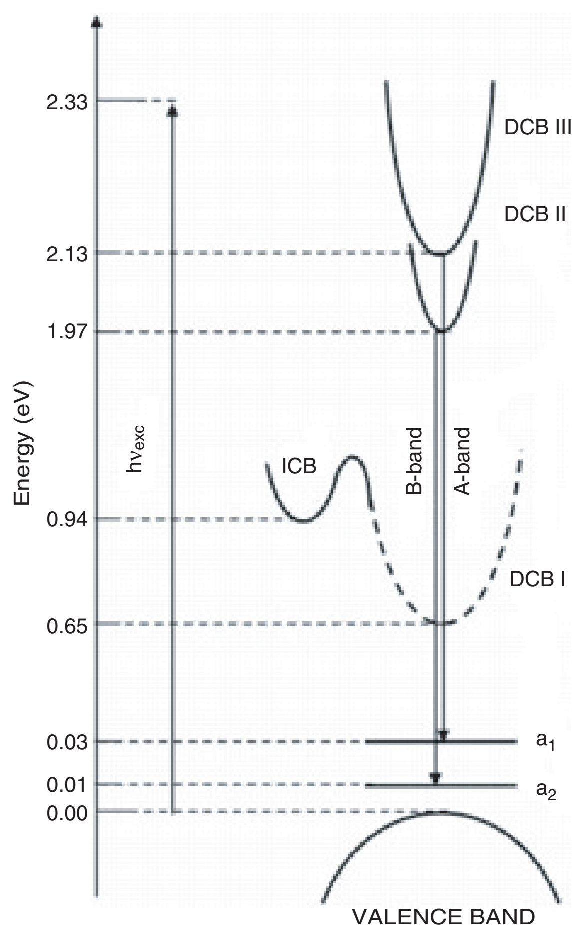

Figure 5. Proposed energy-level diagram of $Tl_4In_3GaSe_8$ at $T = 16$ K.

the red line of the He–Ne laser ($E_{exc} = 1.96$ eV). The presence of the emission bands in the PL spectra at higher energies than the fundamental band gap energy has also been reported for $CuGaTe_2$ ternary crystals [15]. It was proposed that the transitions from a higher conduction band minimum to defect states are responsible for the observed PL bands.

At low excitation intensity ($L < 0.0873$ W cm^{-2}) sufficient to observe the B-band emission (figure 3(a)), the quasi-Fermi level for electrons is located above only the minimum of the second conduction band (figure 5). With increasing excitation intensity ($L \geqslant 0.0873$ W cm^{-2}), the quasi-Fermi level for electrons is shifted and the number of excited electrons is large enough to fill the third conduction band as well, responsible for the observed A-band emission. Therefore, in the PL spectra we observe A-band emission along with the B-band (figure 3(b)). If the transition probability for electrons from the third conduction band to acceptor level $\boldsymbol{a}_1$ is much greater than that for electrons from the second conduction band to acceptor level $\boldsymbol{a}_2$, then, with increasing excitation intensity ($L > 0.4527$ W cm^{-2}), the dominant radiative recombination will occur from the third conduction band (figures 3(b) and 5). The decrease in the B-band intensity with increasing excitation intensity may probably be attributed to the activation of a non-radiative recombination channel. There is no doubt that

further studies are needed to attain a definite solution and/or interpretation of the origin of the B-band intensity decrease.

4. Conclusions

The PL spectra of $Tl_4In_3GaSe_8$ chain crystals as a function of laser excitation intensity and temperature were investigated. Two emission bands centred at 589 nm (2.10 eV, A-band) and 633 nm (1.96 eV, B-band) were observed in the PL spectra at $T = 16$ K. The variations of the spectra with excitation intensity and temperature suggest that the transitions from two upper conduction bands to the acceptor levels with activation energies of 0.03 and 0.01 eV, respectively, can be responsible for the observed emissions. A sublinear increase in the emission band's intensity in $Tl_4In_3GaSe_8$ with excitation intensity confirms our assignment of these bands to free-to-bound recombination. As the crystals studied were not intentionally doped, the acceptor states are thought to originate from uncontrolled impurities and point defects, created during crystal growth.

References

[1] Muller D, Eulenberger G and Hahn H 1973 *Z. Anorg. Allg. Chemie* **398** 207
[2] Gasanly N M 2006 *J. Korean Phys. Soc.* **48** 914
[3] Hanias M, Anagnostopoulos A, Kambas K and Spyridelis J 1989 *Physica* B **160** 154
[4] Rabinal M K, Titus S S K, Asokan S, Gopal E S R, Godzhaev M O and Mamedov N T 1993 *Phys. Status Solidi* b **178** 403
[5] Allakhverdiev K R, Mamedov T G, Salaev E Y and Efendieva I K 1982 *Phys. Status Solidi* b **113** K43
[6] Kilday D G, Niles D W, Margaritondo G and Levy F 1987 *Phys. Rev.* B **35** 660
[7] Gasanly N M, Ragimov A S, Goncharov A F, Melnik N N and Vinogradov E A 1983 *Physica* B and C **115** 381
[8] Mamedov N, Wakita K, Akita S and Nakayama Y 2005 *Japan. J. Appl. Phys.* **44** 709
[9] Guseinov G D, Mooser E, Kerimova E M, Gamidov R S, Alekseev I V and Ismailov M Z 1969 *Phys. Status Solidi* **34** 33
[10] Ellialtioglu S, Mete E, Shaltaf R, Allakhverdiev K, Gashimzade F, Nizametdinova M and Orudzhev G 2004 *Phys. Rev.* B **64** 195118
[11] Orudzhev G, Mamedov N, Uchiki H, Yamamoto N, Iida S, Toyota H, Gojaev E and Gashimzade F 2003 *J. Phys. Chem. Solids* **64** 1703
[12] Orudzhev G S, Godzhaev E M, Kerimova R A and Allakhyarov E A 2006 *Phys. Status Solidi* **48** 42
[13] Okazaki K, Tanaka K, Matsuno J, Fujimori A, Mattheiss L F, Iida S, Kerimova E and Mamedov N 2001 *Phys. Rev.* B **64** 045210
[14] Schmidt T, Lischka K and Zulehner W 1992 *Phys. Rev.* B **45** 8989
[15] Krustok J, Collan H, Hjelt K, Yakushev M, Hill A E, Tomlinson R D, Mandar H and Neumann H 1998 *J. Appl. Phys.* **83** 7867
[16] Jagomagi A, Krustok J, Raudoja J, Grossberg M and Danilson M 2003 *Phys. Status Solidi* b **237** R3
[17] Yu P and Cardona M 1995 *Fundamentals of Semiconductors* (Berlin: Springer) p 343
[18] Ellialtioglu S, Mete E and Yildirim O 2006 at press